Superatomic Nature of Metal Encapsulated Dodecahedrane: The Case of M@C20H20 (M = Li, Na, Mg+)

Isuru Ariyarathna[1]

[1]Auburn University College of Sciences and Mathematics

May 27, 2021

Abstract

The idea of designing unprecedented materials made of superatomic building blocks, motivated the present study on endohedral M@C20H20 (M = Li, Na, Mg+) species. Ground and excited electronic structures of M@C20H20 (M = Li, Na, Mg+) were analyzed by means of high-level quantum calculations. In their ground states, one electron occupies a defuse superatomic s-orbital that lies around the C20H20 cage. These entities populate higher angular momentum p-, d-, f-, g-superatomic orbitals in their low-lying electronic states. The proposed superatomic Aufbau shell model for Li@C20H20 and Na@C20H20 is 1s, 1p, 1d, 2s, 1f, 2p, 2d, 1g, 2f slightly different from that of Mg@C20H20+ which is 1s, 1p, 1d, 2s, 1f, 2p, 2d, 1g, 3s, 2f, 2g, 3p. These introduced superatomic orbital series resemble the Aufbau principle of solvated electron precursors.

1. INTRODUCTION

The concept of atoms or molecules encapsulation in cavities of a host molecule has gained a significant interest in pharmaceutical, food, and material research studies.[1–8] Hydrocarbon cages and fullerenes are suitable candidates for encapsulation of atoms or small molecules. In the past several experimental[9–17] and theoretical[18,19,28–35,20–27] accounts on such fullerene based encapsulated systems are reported. However, experimental studies on atoms or molecules entrapped fully hydrogenated fullerenes are rare. For example, $He@C_{20}H_{20}$ is the only synthesized encapsulated system of $C_{20}H_{20}$ (Dodecahedrane) reported thus far.[36] Due to the lack of experimental studies, the knowledge progression of such $C_{20}H_{20}$based encapsulation systems have mostly been via theoretical studies.[37–41]

The first *ab initio* study on $C_{20}H_{20}$ based encapsulation systems belongs to Disch and Schulman who studied $X@C_{20}H_{20}$ (X = H^+, He, Li^+, Be, Be^+, Be^{2+}, Na^+, Mg^{2+}) species at Hartree-Fock level.[38] According to their analysis He, Be, Be^+, and Na^+encapsulated $C_{20}H_{20}$ are metastable with respect to the corresponding fragments.[38] Moran et al. carried out a comprehensive analysis of geometries, stabilities, and energetics of $X@C_{20}H_{20}$ (X = H, He, Ne, Ar, Li, Li^+, Be, Be^+, Be^{2+}, Na, Na^+, Mg, Mg^+, Mg^{2+}) using B3LYP/6-311+G(d,p) in 2002.[41] They found that X = Be, Be^+, and Be^{2+} encapsulated complexes possess C_{5v} symmetry, where X is located close to an interior pentagonal face of $C_{20}H_{20}$. All the other species bear $I_h$minima.[41] Furthermore, they reported the He, Ne, Li, Li^+, Li^-, Na, Na^+, Be, Be^+, Be^{2+}, Mg, Mg^+, and Mg^{2+} form more stable exohedral complexes with $C_{20}H_{20}$ compared to the corresponding endohedral species.[41]

Interestingly, Li, Na, and Mg encapsulated $C_{20}H_{20}$ species ($M@C_{20}H_{20}$; M = Li, Na, Mg) can be recognized as *"superalkalis"* owing to their lower first ionization energies (IE1s).[41] The rather diffuse nature of the highest occupied molecular orbital (HOMO) is responsible for their lower ionization potentials. Moreover, it may engender the superior electrical conductivity of $Li@C_{20}H_{20}$ predicted by Wang et al.[40] The existing expanded electron cloud of the ground state of each $M@C_{20}H_{20}$ (M = Li, Na, Mg) is nearly spherical resembling an atomic s-orbital. In that sense these molecules are similar to the previously studied*"solvated*

electron precursors" (SEPs), where an SEP is a complex that consists of $M(L)_n$ $^{q+}$ core (M = metal, L = ligand) with one or few diffuse electrons.[42–47]Interestingly, SEPs populate atomic p-, d-, f-, and g-type orbitals in excited states. The exact Aufbau order introduced for the $M(NH_3)_4$ (M = Li, Na) SEPs is 1s, 1p, 1d, 2s, 2p.[42] The implementation of an augmented basis set on terminal H-atoms is critically important for the correct representation of their excited states.[43,44]Specifically, the M:cc-pVTZ, N/O:cc-pVTZ, H:d-aug-cc-pVTZ combination is proven to describe the excited electronic states of SEPs accurately and efficiently.[43,44]

Similar to the SEPs the $M@C_{20}H_{20}$ (M = Li, Na, Mg^+) populate higher angular momentum p-, d-, f-shaped orbitals in low-lying excited electronic states, hence can be recognized as *"superatoms"* . The main goal of the present work is to analyze their ground and excited states adopting high-level *ab initio* calculations. By means of highly accurate electron propagator theory calculations their exact Aufbau models and basis set effects on excitation energies are analyzed. The computational approach and the results of this work are discussed under sections 2 and 3, respectively. Main findings of the study are summarized in section 4.

2. COMPUTATIONAL DETAILS

Geometries of neutral and charged endohedral $M@C_{20}H_{20}$ (M = Li, Na, Mg) species were optimized in I_h symmetry using density functional theory combined with B3LYP functional at aug-cc-pVTZ basis set.[48,49] Their cartesian coordinates and harmonic vibrational frequencies are reported in the Electronic Supplementary Information (ESI) (Tables S1and S2). Single point MP2 (second-order Møller–Plesset perturbation theory)[50] calculations were performed using B3LYP geometries [MP2(FC)//B3LYP] to obtain adiabatic ionization energies (AIEs). AIE of $M@C_{20}H_{20}$ = Energy of optimized $M@C_{20}H_{20}{}^{+/2+}$ - Energy of optimized $M@C_{20}H_{20}$. The unrestricted Hartree-Fock spin contamination for open shell species did not exceed 0.0011. Renormalized partial third-order quasiparticle electron propagator method (P3+)[51–53] was used to obtain vertical ionization energies (VIEs) of $Li@C_{20}H_{20}$, $Na@C_{20}H_{20}$, and $Mg@C_{20}H_{20}$. For this purpose, vertical electron binding energies (VEBE) of $Li@C_{20}H_{20}{}^+$, $Na@C_{20}H_{20}{}^+$, $Mg@C_{20}H_{20}{}^+$, and $Mg@C_{20}H_{20}{}^{2+}$ were calculated (-VEBE = VIE) using the B3LYP optimized geometries of $MC_{20}H_{20}$ (M = Li, Na, Mg).

Excited states of $MC_{20}H_{20}$ (M = Li, Na, Mg^+) were investigated at diagonal second-order approximation (D2), partial third-order quasiparticle (P3), and P3+ electron propagator methods.[51–54] The accuracy of these methods increases in the order of D2, P3, and P3+.[55] These techniques were used to calculate vertical electron attachment energies of $MC_{20}H_{20}$ (M = Li^+, Na^+, Mg^{2+}) and their differences were calculated to obtain vertical excitation energies of $MC_{20}H_{20}$ (M = Li, Na, Mg^+). In each case, B3LYP optimized geometries of $MC_{20}H_{20}$ (M = Li, Na, Mg^+) were employed.

Various correlation consistent basis set combinations [cc-pVTZ ([?]TZ), aug-cc-pVTZ ([?]ATZ), d-aug-cc-pVTZ ([?]DATZ)] were tested to study excited states of $Li@C_{20}H_{20}$.[48,49,56]They are, (1) Li:TZ, C:TZ, H:TZ, (2) Li:TZ, C:TZ, H:ATZ, (3) Li:TZ, C:ATZ, H:TZ, (4) Li:ATZ, C:TZ, H:TZ, (5) Li:TZ, C:ATZ, H:ATZ, (6) Li:ATZ, C:TZ, H:ATZ, (7) Li:ATZ, C:ATZ, H:TZ, (8) Li:ATZ, C:ATZ, H:ATZ, (9) Li:TZ, C:TZ, H:DATZ. Results indicate that the $(9)^{th}$ basis set (Li:TZ, C:TZ, H:DATZ) provides the most accurate results and therefore was used to carry out vertical electron attachment calculations for the $Na@C_{20}H_{20}{}^+$ and $Mg@C_{20}H_{20}{}^{2+}$. The pole strengths related to electron attachment energies of all the species are greater than 0.950.

All calculations were performed using Gaussian 16 package[57]. GaussView[58] and Molden[59] software packages were used to plot Dyson orbitals.

3. RESULTS AND DISCUSSION

3.1 Ground States Properties

$C_{20}H_{20}{}^-$ is not stable with respect to $C_{20}H_{20}$ + e dissociation. So, is it possible for endohedral $M@C_{20}H_{20}$ (M = Li, Na) to have $M^*@C_{20}H_{20}$("*" represents the unpaired electron) electronic structure rather than $M^+@C_{20}H_{20}{}^-$? Based on the findings of this study, the unpaired electron of $M@C_{20}H_{20}$ (M = Li, Na, Mg^+) is delocalized in the periphery of the $[M@C_{20}H_{20}]^+$occupying a pseudo spherical atomic s-type molecular orbital (see Figure 1). This diffuse molecular orbital is doubly occupied in the ground state of $Mg@C_{20}H_{20}$.

The top and side views of endohedral $Li@C_{20}H_{20}$ are illustrated in Figure 1. Each $Li@C_{20}H_{20}$ and $Li@C_{20}H_{20}^{+}$ were optimized at B3LYP and MP2 levels. The MP2 optimized M-C, C-C, and C-H lengths of $Li@C_{20}H_{20}$ are 2.186, 1.560, and 1.090 A, respectively. Corresponding bond distances of $Li@C_{20}H_{20}^{+}$ at the same level are 2.189, 1.562, and 1.086 A. B3LYP optimized parameters of these structures are listed in the Table 1. Evidently, the B3LYP parameters of $Li@C_{20}H_{20}$ and $Li@C_{20}H_{20}^{+}$ are in very good agreement with their MP2 values (see Table 1). Since MP2 geometry optimizations for these species are extremely demanding, only B3LYP optimizations were performed for all other reported species. Going from neutral to charged species, M-C and C-C lengths stretch by ~0.004 A and ~0.002 A, respectively (Table 1). Compared to bare $C_{20}H_{20}$ all the studied encapsulated systems have longer C-C bonds. C-H distances shorten by ~0.005 A going from neutral to charged complexes. Interestingly, we observed a similar pattern for SEPs in the past, i.e., going from $Li(NH_3)_4$, $Be(NH_3)_4$, $Ca(NH_3)_6$, $Mg(H_2O)_6$ SEPs to their corresponding charged complexes M-Ligand bonds elongate but N-H/O-H bonds compress.[42–45] The longest C-H was observed for the $Mg@C_{20}H_{20}$ (1.096 A) and it is only 0.007 A longer than that of $C_{20}H_{20}$. Complexes that do not possess outer diffuse electrons, i.e., $Li@C_{20}H_{20}^{+}$, $Na@C_{20}H_{20}^{+}$, and $Mg@C_{20}H_{20}^{2+}$, have shorter C-H bonds compared to the ones of $C_{20}H_{20}$.

MP2//B3LYP and P3+ IEs of all the species are given in Table 1. Only for $Li@C_{20}H_{20}$ AIE1 obtained by full MP2 geometry optimizations and the values is 2.410 eV. The difference between aforementioned value and the MP2//B3LYP AIE1 of $Li@C_{20}H_{20}$ is only 0.001 eV (see Table 1). This shows that MP2//B3LYP IEs of $M@C_{20}H_{20}$ are reliable. Several basis sets were implemented at P3+ to obtain VIE1 of $Li@C_{20}H_{20}$, i.e., (1) $IE1_{(Li:TZ,\ C:TZ,\ H:TZ)}$ = 1.818 eV, (2) $IE1_{(Li:TZ,\ C:TZ,\ H:ATZ)}$ = 2.373 eV, (3) $IE1_{(Li:TZ,\ C:ATZ,\ H:TZ)}$ = 2.337 eV, (4) $IE1_{(Li:ATZ,\ C:TZ,\ H:TZ)}$ = 2.329 eV, (5) $IE1_{(Li:TZ,\ C:ATZ,\ H:ATZ)}$ = 2.366 eV, (6) $IE1_{(Li:ATZ,\ C:TZ,\ H:ATZ)}$ = 2.350 eV, (7) $IE1_{(Li:ATZ,\ C:ATZ,\ H:TZ)}$ = 2.353 eV, (8) $IE1_{(Li:ATZ,\ C:ATZ,\ H:ATZ)}$ = 2.351 eV, (9) $IE1_{(Li:TZ,\ C:TZ,\ H:DATZ)}$ = 2.350 eV. All the basis sets except (1) have diffuse basis functions and predicted ~2.3 eV IE1.

The IE1s of naked Li (5.392 eV) and Na (5.139 eV) are bigger (approximately by 3 eV) compared to those of $Li@C_{20}H_{20}$ to $Na@C_{20}H_{20}$.[60] The reported B3LYP/6-311+G(d,p) VIE1s of $Li@C_{20}H_{20}$ (2.77 eV), $Na@C_{20}H_{20}$ (2.67 eV), and $Mg@C_{20}H_{20}$ (3.43 eV) by Moran et al.[41] are ~0.4 eV bigger compared to the calculated P3+ values in this study. Since each $Li@C_{20}H_{20}$, $Na@C_{20}H_{20}$, and $Mg@C_{20}H_{20}$ possesses a lower IE1 than that of cesium atom, i.e., experimental $IE1_{Cs}$ = 3.894 eV[60], they can be categorized as superalkalis.[61]

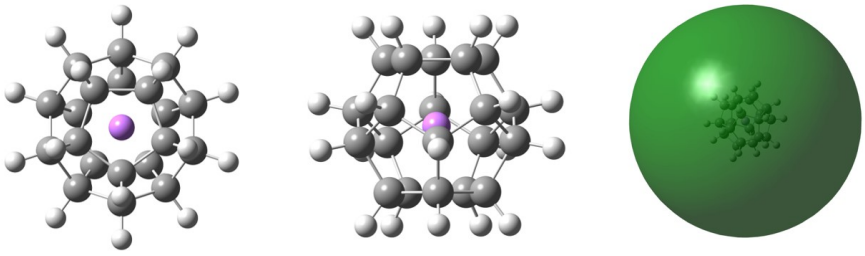

Figure 1. Top view *(a)* , side view *(b)* , and HOMO *(c)* of $Li@C_{20}H_{20}$

Table 1. Optimized bond distances (Å) at B3LYP, relative energies under MP2//B3LYP (ΔE, eV), and negative of vertical electron binding energies (-VEBE, eV) obtained with P3+ of $MC_{20}H_{20}$ species. B3LYP and MP2 results obtained under M:ATZ, C:ATZ, H:ATZ basis set. P3+ values are from M:TZ, C:TZ, H:DATZ set.

Species	Geometric parameters	Geometric parameters	Geometric parameters	ΔE (MP2)	-VEBE (P3+)
	M-C	C-C	C-H		

Species	Geometric parameters	Geometric parameters	Geometric parameters	ΔE (MP2)	-VEBE (P3+)
$Li@C_{20}H_{20}$	2.191	1.564	1.089	0.000	0.000
$Li@C_{20}H_{20}^{+}$	2.194	1.566	1.085	2.411	2.350
$Na@C_{20}H_{20}$	2.215	1.581	1.088	0.000	0.000
$Na@C_{20}H_{20}^{+}$	2.218	1.583	1.083	2.315	2.270
$Mg@C_{20}H_{20}$	2.215	1.581	1.096	0.000	0.000
$Mg@C_{20}H_{20}^{+}$	2.220	1.584	1.090	3.250	3.029
$Mg@C_{20}H_{20}^{2+}$	2.220	1.585	1.082	9.603	9.010
$C_{20}H_{20}$	-	1.551	1.089	-	-

3.2 Excited States Analysis

The electron present in the superatomic s-orbital of the ground state of $M@C_{20}H_{20}$ (M = Li, Na, Mg^{+}) populates p-, d-, f-, g-superatomic orbitals in excited states. *Ab initio* electron propagator theory methods are ideal to study excited states of such systems efficiently with high accuracy.[42,43,47] Using D2, P3, and P3+ levels of this theory excitation energies of $M@C_{20}H_{20}$(M = Li, Na, Mg^{+}) were obtained by calculating the vertical electron affinities of $M@C_{20}H_{20}$(M = Li^{+}, Na^{+}, Mg^{2+}). Computed electron attachment energies and corresponding pole strengths of all the species are included in the Tables S3, S5, S7, S9, S11, S13, S15, S17, S19, S21, and S23.

3.2.1. $Li@C_{20}H_{20}$

In the past we found that M:TZ, N/O:TZ, H:DATZ basis set is capable of providing accurate excitation energies for SEPs.[43,44]A similar basis set combination [M:TZ, C:TZ, H:DATZ; basis set (9)] was adopted to study excited states of $Li@C_{20}H_{20}$ under D2, P3, and P3+ levels of theory. Under this basis set ten excited states reside within its IE1 limit (see the values reported in the Table 2). The first excited state ($^2T_{1u}$) lies 0.398 eV above the ground state at P3+ level and the unpaired electron occupies a p-type superatomic orbital (see Figure 2). The second excited state (1^2H_g at 0.956 eV) bear $1d^1$ superatomic electron configuration. After that this electron jumps to 2s and 1f superatomic orbitals. Note thatI_h symmetry splits 1f or 1g shells into two non-degenerate components. Specifically, the $1f^1$electronic configuration caries by the 1^2T_{2u} (1.417 eV) and 1^2G_u (1.477 eV) states. The 2p, 2d 1g, and 2f shaped orbitals are occupied in next five excited states (1.460-2.247 eV range). The $1g^1$ configuration belongs to two non-degenerate ^2G_g and^2H_g states. The^2G_g state of $Li@C_{20}H_{20}$ lies at 1.914 eV but the^2H_g is not bound. Overall, the observed superatomic Aufbau principle of $Li@C_{20}H_{20}$ at all levels is 1s, 1p, 1d, 2s, 1f, 2p, 2d, 1g, 2f. Shapes of selected 1s, 1p, 1d, 1f, and 1g superatomic orbitals are given in Figure 2. Interestingly, it is identical to the Aufbau rule that we introduced for $Be(NH_3)_4^{+}$ SEP (1s, 1p, 1d, 2s, 1f, 2p, 2d).[43] In overall, P3+ values are lower than D2 but bigger than P3 numbers for all the excitations except for the 1s - 2s transition (see Table 2). The excitation energy differences between P3+ and P3 are small (0.003-0.008 eV). The discrepancy between P3+ and D2 energies are within 0.014-0.057 eV.

Several other basis sets were also probed for $Li@C_{20}H_{20}$ (see the values under basis set (1) - (8) of Table 2). Only the P3+ vertical excitation energies are listed in Table 2 and corresponding D2 and P3 values are listed in the ESI (Table S4, S6, S8, S10, S12, S14, S16, and S18). In all the cases the first excitation corresponds to 1s - 1p transition. The smallest basis set [basis set (1)] underestimates the first excitation energy by 0.225 eV compared to the basis set (9). Interestingly, at the basis set (1) only one more excited state is bound. The second excited state is at 1.285 eV and the shape of the populating orbital does not resemble a superatomic orbital. The addition of augmented set of basis functions to H-atoms increased the number of bound excited states up to six (see the values under basis set (2) in Table 2). The 1s - 1p transition at basis set (2) is 0.033 eV greater than the corresponding value at basis set (9). Similar to the basis set (9), the second transition at the basis set (2) is 1s - 1d but higher in energy (0.956 vs 1.147 eV). At basis set (2) the orbital that populates the third excited state does not resemble a superatomic orbital shape (see b_2 in Table 2). After that the electron promotes to 1f (1^2T_{2u} and 1^2G_u) and 2s superatomic orbitals. Under the

basis set (3) 1s - non-superatomic electron transitions are absent. The observed orbital model at this level is 1s, 1p, 1d, 1f, 2p which is different from the one predicted by bigger basis set (9). Similarly, at basis set (4) only five excited states are bound. Basis set (5) predicts three 1s - non-superatomic excitations that give rise to 2^2A_g, 1^2T_{2u}, and 2^2T_{1u} states. Under the basis sets (6) and (7) the electron populates 1s, 1p, 1d, 2s, 2p, 1f superatomic orbitals in energy order with only one non-superatomic state.

Even though the basis set (8) has more basis functions than basis set (9) it describes only six bound excited states, and the orbital order is 1s, 1p, 1d, 2s, 2p, 1f. This shows the importance of doubly augmentation on H-atoms for accurate representation of excited states of these systems. Based on this conclusion the basis set (9) was applied to study excited states of $Na@C_{20}H_{20}$ and $Mg@C_{20}H_{20}{}^{+}$.

Table 2. Calculated vertical excitation energies (eV) of $Li@C_{20}H_{20}$ by electron propagator methods under various basis sets. States are ordered according to P3+ excitation energies obtained at Li:TZ, C:TZ, H:DATZ set [basis set (9)] and collected into quasi-degenerate, superatomic shells.

State	Superatomic shell		Basis set	Basis set	Basis set	Basis set	Bas
			9	9	9	1	2
		Li	TZ	TZ	TZ	TZ	TZ
		C	TZ	TZ	TZ	TZ	TZ
		H	DATZ	DATZ	DATZ	TZ	AT
			1270 [a]	1270 [a]	1270 [a]	910 [a]	109
			Excitation energies	Excitation energies	Excitation energies	Excitation energies	Exc
			D2	P3	P3+	P3+	P3
1^2A_g	1^2S		0.000	0.000	0.000	0.000	0.0
1^2T_{1u}	1^2P		0.426	0.394	0.398	0.173	0.4
1^2H_g	1^2D		1.007	0.949	0.956	-	1.1
2^2A_g	2^2S		1.262	1.279	1.276	-	2.2
1^2T_{2u}	1^2F		1.469	1.410	1.417	-	1.7
1^2G_u	1^2F		1.534	1.469	1.477	-	1.8
2^2T_{1u}	2^2P		1.483	1.457	1.460	b_1	b_2
2^2H_g	2^2D		1.846	1.798	1.804		
1^2G_g	1^2G		1.971	1.906	1.914		
2^2T_{2u}	2^2F		2.109	2.076	2.080		
2^2G_u	2^2F		2.298	2.240	2.247		
3^2T_{1u}	-						

a = Total number of basis functions of the basis set.

b_1 = 1.285 eV, b_2 = 1.659 eV, b_4 = 1.625 eV, b_{51} = 1.791 eV, b_{52} = 1.614 eV,b_{53} = 2.156 eV, b_6 = 1.806 eV, and b_7 = 1.851 eV vertical excitation energies do not correspond to superatomic shells.

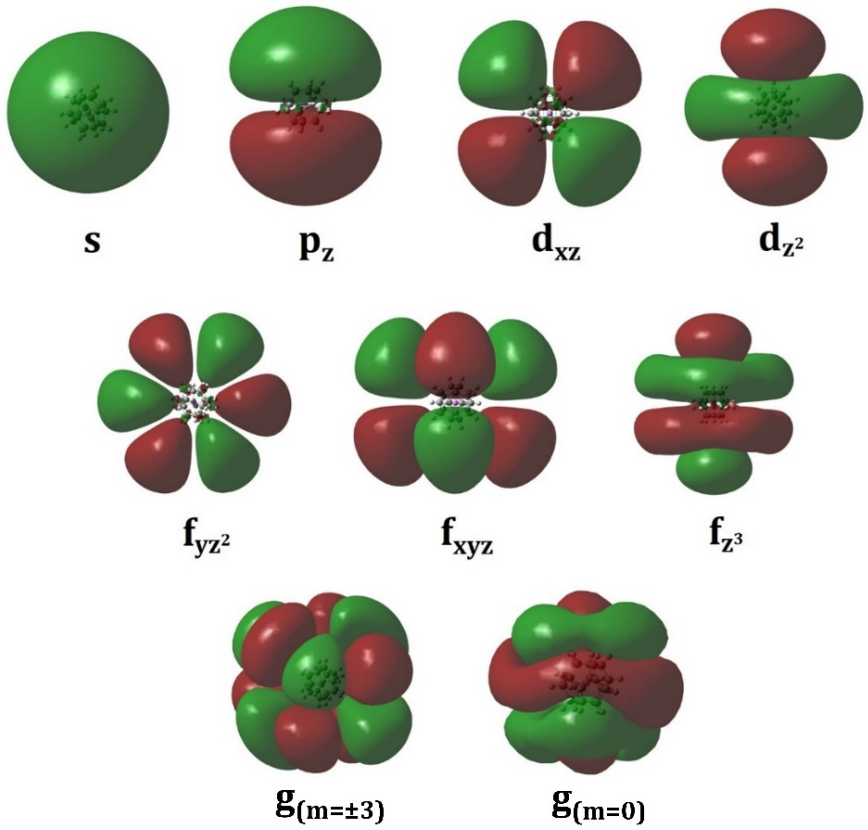

Figure 2. Dyson orbitals correspond to vertical electron attachment of $Li@C_{20}H_{20}^{+}$ (Li:TZ, C:TZ, H:DATZ basis set). Dyson orbitals of $Li@C_{20}H_{20}^{+}$, $Na@C_{20}H_{20}^{+}$, and $Mg@C_{20}H_{20}^{2+}$ have identical shapes.

3.2.2. $Na@C_{20}H_{20}$ and $Mg@C_{20}H_{20}^{+}$

The superatomic shell series of $Na@C_{20}H_{20}$ is identical to the $Li@C_{20}H_{20}$ (see Table 3). The first excitation energy of $Na@C_{20}H_{20}$ is approximately 5.5 times smaller than that of Na atom (0.382 vs 2.10 eV).[62] Compared to $Li@C_{20}H_{20}$, the excitation energies of $Na@C_{20}H_{20}$ are lower by 0.016-0.085 eV at P3+ level. This is consistent with what we have seen for $Li(NH_3)_4$ and $Na(NH_3)_4$ superatoms where the excitation energies of the former is greater than the latter by 0.06-0.15 eV.[42] Similar to the $Li@C_{20}H_{20}$, the P3+ excitation energies are greater than P3 but lower than D2, except for the 1s - 2s transition. For all the states P3 and P3+ values are nearly identical (see Table 3).

$Mg@C_{20}H_{20}^{+}$ has higher excitation energies compared to $Na@C_{20}H_{20}$ because of the greater Coulombic attraction between the charged center ($Mg@C_{20}H_{20}^{2+}$) and the diffuse electron. The shell model of $Mg@C_{20}H_{20}^{+}$ is slightly different from the one of $Li@C_{20}H_{20}$ or $Na@C_{20}H_{20}$. Specifically, up to 1g it is identical to the $Li@C_{20}H_{20}$ or $Na@C_{20}H_{20}$. Unlike $Li@C_{20}H_{20}$ and $Na@C_{20}H_{20}$, both ^2G_g and ^2H_g of 1g of $Mg@C_{20}H_{20}^{+}$ are bound. For $Mg@C_{20}H_{20}^{+}$ case the 3s populates after the 1g. Notice that 3s shell does not populate in either $Li@C_{20}H_{20}$ or $Na@C_{20}H_{20}$. After that 2f, 2g, 3p, and 3f superatomic orbitals are being populated. Within the considered 0.000-4.782 eV range, only ^2G_g of 2g and $^2T_{2u}$ of 3f are bound. Overall, the introduced shell model for $Mg@C_{20}H_{20}^{+}$ is 1s, 1p, 1d, 2s, 1f, 2p, 2d, 1g, 3s, 2f, 2g, 3p, 3f.

Table 3. The ten lowest vertical excitation energies (eV) for $Na@C_{20}H_{20}$ at the D2, P3, and P3+ levels of theory with the Na:TZ, C:TZ, H:DATZ basis sets. The states are ordered according to P3+ excitation energies and collected into quasi-degenerate, superatomic shells.

State	Superatomic shell	Excitation energy	Excitation energy	Excitation energy
		D2	P3	P3+
1^2A_g	1^2S	0.000	0.000	0.000
1^2T_{1u}	1^2P	0.405	0.378	0.382
1^2H_g	1^2D	0.914	0.872	0.878
2^2A_g	2^2S	1.243	1.254	1.253
1^2T_{2u}	1^2F	1.373	1.330	1.336
1^2G_u	1^2F	1.439	1.391	1.397
2^2T_{1u}	2^2P	1.429	1.404	1.408
2^2H_g	2^2D	1.752	1.720	1.725
1^2G_g	1^2G	1.875	1.827	1.833
2^2T_{2u}	2^2F	2.008	1.993	1.995
2^2G_u	2^2F	2.201	2.159	2.165

Table 4. The fifteen lowest vertical excitation energies (eV) for $Mg@C_{20}H_{20}^+$ at the D2, P3, and P3+ levels of theory with the Mg:TZ, C:TZ, H:DATZ basis sets. The states are ordered according to P3+ excitation energies and collected into quasi-degenerate, superatomic shells.

Final State	superatomic shell	Excitation energy	Excitation energy	Excitation energy
		D2	P3	P3+
1^2A_g	1^2S	0.000	0.000	0.000
1^2T_{1u}	1^2P	1.323	1.099	1.134
1^2H_g	1^2D	2.188	1.912	1.954
2^2A_g	2^2S	2.553	2.480	2.487
1^2T_{2u}	1^2F	2.524	2.283	2.320
1^2G_u	1^2F	3.119	2.816	2.861
2^2T_{1u}	2^2P	3.420	3.166	3.204
2^2H_g	2^2D	3.795	3.514	3.556
1^2G_g	1^2G	3.921	3.610	3.656
3^2H_g	1^2G	3.642	3.422	3.456
3^2A_g	3^2S	3.448	3.588	3.556
2^2T_{2u}	2^2F	3.960	3.697	3.737
2^2G_u	2^2F	4.314	4.010	4.055
2^2G_g	2^2G	4.703	4.401	4.446
3^2T_{1u}	3^2P	4.871	4.672	4.702
3^2T_{2u}	3^2F	5.025	4.739	4.782

4. CONCLUSIONS

High-level quantum calculations were performed to study ground and excited states of endohedral $M@C_{20}H_{20}$ (M = Li, Na, Mg^+). Ground state of each $Li@C_{20}H_{20}$, $Na@C_{20}H_{20}$, and $Mg@C_{20}H_{20}^+$ has an electron in a pseudo spherical s-type orbital positioned around $Li@C_{20}H_{20}^+$, $Na@C_{20}H_{20}^+$, and $Mg@C_{20}H_{20}^{2+}$ skeletons. In excited states they populate higher angular momentum p-, d-, f-, g-type superatomic orbitals. Excited states of $Li@C_{20}H_{20}$ were investigated under several basis sets. M:cc-pVTZ, C:cc-pVTZ, H:d-aug-cc-pVTZ combination accurately represent ground and excited electronic structures of these superatoms. The proposed shell model of $Li@C_{20}H_{20}$ and $Na@C_{20}H_{20}$ is 1s, 1p, 1d, 2s, 1f, 2p, 2d, 1g, 2f. The series of $Mg@C_{20}H_{20}^+$ is 1s, 1p, 1d, 2s, 1f, 2p, 2d, 1g, 3s, 2f, 2g, 3p. Excitation energies of $Li@C_{20}H_{20}$ are bigger than $Na@C_{20}H_{20}$ but lower compared to the $Mg@C_{20}H_{20}^+$. We believe these findings will be useful for future studies on similar superatomic systems.

5. CONFLICTS OF INTEREST

There are no conflicts to declare.

6. ACKNOWLEDGEMENTS

This work was completed with resources provided by the Alabama supercomputer and the National Energy Research Scientific Computing Center (NERSC), a U.S. Department of Energy Office of Science User Facility operated under Contract No. DE-AC02-05CH11231.

7. REFERENCES

1. X. Wang, J. Feng, Y. Bai, Q. Zhang, Y. Yin, *Chem. Rev.* ,**2016** , 116, 10983.

2. E. Assadpour, S. Mahdi Jafari, *Crit. Rev. Food Sci. Nutr.* ,**2019** , 59, 3129.

3. M. G. Bah, H. M. Bilal, J. Wang, *Soft Matter* , **2020** , 16, 570.

4. I. R. Ariyarathna, R. M. P. I. Rajakaruna, D. N. Karunaratne,*Food Control* , **2017** , 77, 251.

5. I. Katouzian, S. M. Jafari, *Trends Food Sci. Technol.* ,**2016** , 53, 34.

6. C. Tomaro-Duchesneau, S. Saha, M. Malhotra, I. Kahouli, S. Prakash,*J. Pharm.* , **2013** , 2013, 1.

7. D. N. Karunaratne, D. A. Surandika Siriwardhana, I. R. Ariyarathna, R. M. P. Indunil Rajakaruna, F. T. Banu, V. Karunaratne, in*Nutrient Delivery* , Elsevier, **2017** , pp. 653.

8. D. N. Karunaratne, I. R. Ariyarathna, D. Welideniya, A. Siriwardhana, D. Gunasekera, V. Karunaratne, *Curr. Nanomedicine* , **2017** , 7, 84.

9. J. R. Heath, S. C. O'Brien, Q. Zhang, Y. Liu, R. F. Curl, F. K. Tittel, R. E. Smalley, *J. Am. Chem. Soc.* , **1985** , 107, 7779.

10. M. Saunders, H. A. Jimenez-Vazquez, R. J. Cross, R. J. Poreda,*Science (80-.).* , **1993** , 259, 1428.

11. M. Saunders, H. A. Jiménez-Vázquez, R. J. Cross, S. Mroczkowski, D. I. Freedberg, F. A. L. Anet, *Nature* , **1994** , 367, 256.

12. T. Almeida Murphy, T. Pawlik, A. Weidinger, M. Höhne, R. Alcala, J.-M. Spaeth, *Phys. Rev. Lett.* , **1996** , 77, 1075.

13. C. Knapp, K.-P. Dinse, B. Pietzak, M. Waiblinger, A. Weidinger,*Chem. Phys. Lett.* , **1997** , 272, 433.

14. B. Pietzak, M. Waiblinger, T. A. Murphy, A. Weidinger, M. Höhne, E. Dietel, A. Hirsch, *Chem. Phys. Lett.* , **1997** , 279, 259.

15. T. Wakahara, Y. Matsunaga, A. Katayama, Y. Maeda, M. Kako, T. Akasaka, M. Okamura, T. Kato, Y.-K. Choe, K. Kobayashi, S. Nagase, H. Huang, M. Ata, *Chem. Commun.* , **2003** , 3, 2940.

16. T. Peres, B. Cao, W. Cui, A. Khong, R. J. Cross, M. Saunders, C. Lifshitz, *Int. J. Mass Spectrom.* , **2001** , 210–211, 241.

17. T. Suetsuna, N. Dragoe, W. Harneit, A. Weidinger, H. Shimotani, S. Ito, H. Takagi, K. Kitazawa, *Chem. - A Eur. J.* , **2002** , 8, 5079.

18. C. I. Williams, M. A. Whitehead, L. Pang, *J. Phys. Chem.* ,**1993** , 97, 11652.

19. J. Cioslowski, *J. Am. Chem. Soc.* , **1991** , 113, 4139.

20. F. Uhlík, Z. Slanina, S.-L. Lee, B.-C. Wang, L. Adamowicz, S. Nagase, *J. Comput. Theor. Nanosci.* , **2015** , 12, 959.

21. Z. Slanina, F. Uhlík, X. Lu, T. Akasaka, K. H. Lemke, T. M. Seward, S. Nagase, L. Adamowicz, *Fullerenes, Nanotub. Carbon Nanostructures* , **2016** , 24, 1.

22. Z. Slanina, F. Uhlík, S. Nagase, X. Lu, T. Akasaka, L. Adamowicz,*ChemPhysChem* , **2016** , 17, 1109.

23. Z. Slanina, F. Uhlík, S. Nagase, T. Akasaka, L. Adamowicz, X. Lu,*ECS J. Solid State Sci. Technol.* , **2017** , 6, M3113.

24. Z. Slanina, F. Uhlík, S. Nagase, T. Akasaka, L. Adamowicz, X. Lu,*Fullerenes, Nanotub. Carbon Nanostructures* , **2017** , 25, 624.

25. Z. Y. Wang, K. H. Su, H. Q. Fan, Y. L. Li, Z. Y. Wen, *Mol. Phys.* , **2008** , 106, 703.

26. M. Khatua, S. Pan, P. K. Chattaraj, *Chem. Phys. Lett.* ,**2014** , 610–611, 351.

27. M. Gonzalez, S. Lujan, K. A. Beran, *Comput. Theor. Chem.* ,**2017** , 1119, 32.

28. Z. Slanina, F. Uhlík, L. Adamowicz, S. Nagase, *Mol. Simul.* ,**2005** , 31, 801.

29. C. N. Ramachandran, N. Sathyamurthy, *Chem. Phys. Lett.* ,**2005** , 410, 348.

30. Z. Slanina, S. Nagase, *Mol. Phys.* , **2006** , 104, 3167.

31. O. Shameema, C. N. Ramachandran, N. Sathyamurthy, *J. Phys. Chem. A* , **2006** , 110, 2.

32. Z. Slanina, P. Pulay, S. Nagase, *J. Chem. Theory Comput.* ,**2006** , 2, 782.

33. A. P. Mazurek, N. Sadlej-Sosnowska, *Int. J. Quantum Chem.* ,**2011** , 111, 2398.

34. A. Varadwaj, P. R. Varadwaj, *Chem. - A Eur. J.* ,**2012** , 18, 15345.

35. A. B. Farimani, Y. Wu, N. R. Aluru, *Phys. Chem. Chem. Phys.* ,**2013** , 15, 17993.

36. R. J. Cross, M. Saunders, H. Prinzbach, *Org. Lett.* ,**1999** , 1, 1479.

37. D. A. Dixon, D. Deerfield, G. D. Graham, *Chem. Phys. Lett.* ,**1981** , 78, 161.

38. R. L. Disch, J. M. Schulman, *J. Am. Chem. Soc.* ,**1981** , 103, 3297.

39. Z. Chen, H. Jiao, D. Moran, A. Hirsch, W. Thiel, P. von R. Schleyer,*J. Phys. Chem. A* , **2003** , 107, 2075.

40. Y.-P. An, C.-L. Yang, M.-S. Wang, X.-G. Ma, D.-H. Wang, *J. Phys. Chem. C* , **2009** , 113, 15756.

41. D. Moran, F. Stahl, E. D. Jemmis, H. F. Schaefer, P. V. R. Schleyer,*J. Phys. Chem. A* , **2002** , 106, 5144.

42. I. R. Ariyarathna, F. Pawłowski, J. V. Ortiz, E. Miliordos,*Phys. Chem. Chem. Phys.* , **2018** , 20, 24186.

43. I. R. Ariyarathna, S. N. Khan, F. Pawłowski, J. V. Ortiz, E. Miliordos, *J. Phys. Chem. Lett.* , **2018** , 9, 84.

44. I. R. Ariyarathna, E. Miliordos, *Phys. Chem. Chem. Phys.* ,**2019** , 21, 15861.

45. I. R. Ariyarathna, N. M. S. Almeida, E. Miliordos, *J. Phys. Chem. A* , **2019** , 123, 6744.

46. I. R. Ariyarathna, E. Miliordos, *Phys. Chem. Chem. Phys.* ,**2020** , 22, 22426.

47. I. R. Ariyarathna, F. Pawłowski, J. V. Ortiz, E. Miliordos, *J. Phys. Chem. A* , **2020** , 124, 505.

48. B. P. Prascher, D. E. Woon, K. A. Peterson, T. H. Dunning, A. K. Wilson, *Theor. Chem. Acc.* , **2011** , 128, 69.

49. R. A. Kendall, T. H. Dunning, R. J. Harrison, *J. Chem. Phys.* ,**1992** , 96, 6796.

50. C. Møller, M. S. Plesset, *Phys. Rev.* , **1934** , 46, 618.

51. J. V. Ortiz, *Int. J. Quantum Chem.* , **2005** , 105, 803.

52. J. V. Ortiz, *Wiley Interdiscip. Rev. Comput. Mol. Sci.* ,**2013** , 3, 123.

53. H. H. Corzo, J. V. Ortiz, in *Advances in Quantum Chemistry* , Elsevier, **2017** , pp. 267.

54. J. Linderberg, Y. Öhrn, *Propagators in Quantum Chemistry* , John Wiley & Sons, New Jersey, **2004** .

55. O. Dolgounitcheva, M. Díaz-Tinoco, V. G. Zakrzewski, R. M. Richard, N. Marom, C. D. Sherrill, J. V. Ortiz, *J. Chem. Theory Comput.* ,**2016** , 12, 627.

56. T. H. Dunning, *J. Chem. Phys.* , **1989** , 90, 1007.

57. M. J. Frisch, G. W. Trucks, H. B. Schlegel, G. E. Scuseria, M. A. Robb, J. R. Cheeseman, G. Scalmani, V. Barone, G. A. Petersson, H. Nakatsuji, X. Li, M. Caricato, A. V. Marenich, J. Bloino, B. G. Janesko, R. Gomperts, B. Mennucci, H. P. Hratchian, J. V. Ortiz, A. F. Izmaylov, J. L. Sonnenberg, D. Williams-Young, F. Ding, F. Lipparini, F. Egidi, J. Goings, B. Peng, A. Petrone, T. Henderson, D. Ranasinghe, V. G. Zakrzewski, J. Gao, N. Rega, G. Zheng, W. Liang, M. Hada, M. Ehara, K. Toyota, R. Fukuda, J. Hasegawa, M. Ishida, T. Nakajima, Y. Honda, O. Kitao, H. Nakai, T. Vreven, K. Throssell, J. A. Montgomery, Jr., J. E. Peralta, F. Ogliaro, M. J. Bearpark, J. J. Heyd, E. N. Brothers, K. N. Kudin, V. N. Staroverov, T. A. Keith, R. Kobayashi, J. Normand, K. Raghavachari, A. P. Rendell, J. C. Burant, S. S. Iyengar, J. Tomasi, M. Cossi, J. M. Millam, M. Klene, C. Adamo, R. Cammi, J. W. Ochterski, R. L. Martin, K. Morokuma, O. Farkas, J. B. Foresman, and D. J. Fox, Gaussian, Inc., Wallingford CT, 2016.

58. R. Dennington, T. A. Keith, J. M. Millam, *Gaussview version 6* , Shawnee Mission KS, **2016** .

59. G. Schaftenaar, J.H. Noordik, *J. Comput. Aided. Mol. Des.* ,**2000** , 14, 123.

60. D. R. Lide, *CRC Handbook of Chemistry and Physics* , CRC press, New York, 93rd edn., **2012** .

61. G. L. Gutsev, A. I. Boldyrev, *Chem. Phys. Lett.* ,**1982** , 92, 262.

62. A. Kramida, Y. Ralchenko, J. Reader, NIST ASD Team., NIST Atomic Spectra Database (version 5.4), Vol. 2016, National Institute of Standards and Technology, Gaithersburg, MD, 2016. http://physics.nist.gov/asd.